

Biosynthesis of copper oxide nanoparticles using *Caesalpinia sappan* extract: *In vitro* evaluation of antifungal and antibiofilm activities against *Candida albicans*

Mathurada Sasarom¹, Phenphichar Wanachantararak², Pisaisit Chaijareenont^{2,3}, Siriporn Okonogi^{1,3,*}

¹ Faculty of Pharmacy, Chiang Mai University, Chiang Mai, Thailand;

² Faculty of Dentistry, Chiang Mai University, Chiang Mai, Thailand;

³ Center of Excellent in Pharmaceutical Nanotechnology, Chiang Mai University, Chiang Mai, Thailand.

SUMMARY Synthesis of nanoparticles using natural organic substances has attracted more attention due to avoiding inorganic toxicity. This work aimed to synthesize copper oxide nanoparticles (CuONPs) using *Caesalpinia sappan* heartwood extract as a reducing agent. The effects of pH of synthesis reaction were investigated. The obtained CuONPs were characterized using UV-visible spectroscopy, Fourier transform infrared spectroscopy, scanning electron microscopy, and energy dispersive X-ray spectroscopy. Their particle size, size distribution, and zeta potential were determined using photon correlation spectrophotometry. *Candida albicans* is a major cause of chronic fungal infections due to its biofilms leading to severe drug resistance problems. In this study, *in vitro* antifungal and antibiofilm activities as well as killing kinetics of the synthesized CuONPs against *C. albicans* were investigated. Additionally, fungal biofilm was observed by using confocal laser scanning microscopy. The results showed that the pH of the synthesis reaction played an important role in the physicochemical properties and antifungal activities of the obtained CuONPs. CuONPs synthesized at pH 10 and 12 showed the relatively small and narrow size distribution with high negative zeta potential and time-dependent killing kinetics. Confocal laser scanning microscopy confirms obvious fungal biofilm reduction and increased fungal cell death after exposure to CuONPs. These findings suggest the optimal pH of CuONPs synthesis using *C. sappan* extract as a reducing agent. The results on antifungal and antibiofilm activities indicate that the obtained CuONPs can be a promising agent for treating fungal infection.

Keywords *Caesalpinia sappan*, green synthesis, copper oxide nanoparticles, antifungal activity, antibiofilm activity

1. Introduction

Candida albicans is a normal flora microorganism in humans. However, certain factors, e.g., diet, medications, pH, and the human immune system, can modulate favorable conditions for its overgrowth and turn *C. albicans* into an insidious species and being the main cause of many fungal infections in humans and animals (1). Moreover, *C. albicans* can form biofilms that protect them from harmful substances and thus survive in various conditions and become resistant to antifungal drugs. Biofilm formation of *C. albicans* begins with the adherence of cells to a solid surface. The biofilms then develop from cell proliferation and early-stage filamentation of the adhered cells, resulting in a complex

network of many layers. The developed biofilms consist of several types of cells encased in an extracellular matrix (2). Finally, the biofilms appear thick appearance to protect the microorganisms inside and make the treatment of these infections difficult (3). In the oral cavity, *C. albicans* biofilms formed on implanted medical devices can act as a reservoir for pathogenic cells (4). In denture-wearing patients, *C. albicans* is associated with denture acrylic surfaces to form biofilms (5). These biofilms can cause antimicrobial resistance and bloodstream infection leading to invasive systemic infections (candidemia). These infections have increased in modern clinical practice, especially in immunocompromised patients such as human immunodeficiency virus-infected patients and cancer patients who receive chemotherapy (6).

For this reason, the biofilm formation of *C. albicans* is a serious clinical effect as they can cause significant resistance to antifungal therapy by limiting the penetration of antibiotics and host immune response (7).

Nanotechnology is an important field of modern scientific research due to its wide range of applications. In the medical field, nanotechnology has been applied to the production and application of nanosized particles (nanoparticles) for diagnosis and therapeutics. Novel techniques and methods are continuously studied to produce different types of nanoparticles. Metal nanoparticles are one of those nanoparticles that are increasingly used in the biomedical field. (8). Among metal nanoparticles, copper oxide nanoparticles (CuONPs) have received great interest for many applications, including in the medical field due to their cost-effectiveness, economical attractiveness, promising nontoxicity, and easy preparation. They are used to manufacture electrical and electronic devices, catalysts in various chemical processes, cancer cell treatment applications and antimicrobial formulations (9–12). Furthermore, they show antimicrobial activity against various fungi, which are pathogenic for both agriculture and humans. Colonization of *Candida* spp. has been reported in many studies and some of them are resistant to antifungal agents (13). Interestingly, CuONPs have been reported to have a high potential to inhibit several strains of oral bacteria and fungi, especially *C. albicans* (14). Therefore, CuONPs can be a good candidate in various applications for health and safety issues.

The significant properties required for nanoparticles to be used in biological applications are high biocompatibility, bioactivity, bioavailability, and less toxicity as well as cost-effectiveness (15). However, these properties are rare in metal nanoparticles prepared from inorganic chemical-mediated synthesis. Therefore, there is a need for an environmentally and economically feasible way to synthesize these metal nanoparticles. Biosynthesis with the help of plant extracts, microorganisms, and algae, has attracted much attention (16–18). Among them, plant extracts have gained more selection than others for the biosynthesis of metal nanoparticles due to biocompatibility with biomedical applications, easy handling, accessibility, simplicity, environmentally friendly and nontoxic (19,20). In addition, phytochemical assisted synthesis of metal nanoparticles is an inexpensive and cost-effective approach (21). Different plant extracts have been used to prepare CuONPs (22,23). However, biosynthesis of CuONPs using *C. Sappan* extract has not been reported elsewhere.

C. Sappan is a plant of the Leguminosae family and distributed in Southeast Asia. The heartwood of *C. Sappan* is used as a coloring agent in food, beverages, cosmetics, and curative agents for treating arthritis, antidiabetic and skin infections (24). In many studies, the extract of *C. sappan* showed important biological activities such as antimicrobial (25), anti-

inflammatory (26) and antioxidant activities (27). The heartwood of *C. sappan* consists of several phenolic components, including xanthone, coumarin, flavones, homoisoflavonoids, and brazilin (28). It has been reported that different phytochemicals in plant extracts play a significant role in the reduction process and capping of the synthesized metal nanoparticles (29). Since different plant extract consists of different phytochemicals, thus the physicochemical properties and activities of CuONPs obtained from different plant extract are different. In addition, synthesis-related factors such as pH and temperature also play an important role in controlling the quality and quantity of the nanoparticles (18,30). Therefore, it is challenging to investigate the physicochemical properties and antifungal activities against *C. albicans* of CuONPs synthesized using *C. sappan* extract as a reducing agent in various pH media.

2. Materials and Methods

2.1. Materials

C. albicans DMST 5815 was purchased from the National Institute of Health, Department of Medical Sciences, Ministry of Public Health, Thailand. Copper (II) sulfate pentahydrate salt ($\text{CuSO}_4 \cdot 5\text{H}_2\text{O}$) was purchased from Merck (Darmstadt, Germany). Sodium hydroxide (NaOH) and hydrochloric acid (HCl) were from RCI Labscan (Bangkok, Thailand). Sabouraud dextrose broth (SDB) and sabouraud dextrose agar (SDA) were purchased from Hime-dialabs (Mumbai, India). Tystatin (Nystatin) was from T.O. Pharma Co., LTD (Bangkok, Thailand). Other chemicals and solvents are of analytical grade.

2.2. Preparation of the extract

C. sappan was collected from the northern area of Thailand in January 2021. It was identified by a botanist in the botanical herbarium of the Faculty of Pharmacy, Chiang Mai University to obtain the reference voucher specimen (No. 002276). The heartwood of *C. sappan* was dried in an oven and ground to become a fine powder. To prepare a *C. sappan* aqueous extract, 5 g of the heartwood powder was mixed with 50 mL of water. Subsequently, the mixture was stirred at 500 rpm overnight. The extract was then filtered through Whatman's No.1 filter paper. The filtrate was centrifuged at $3000 \times g$ for 10 min to eliminate precipitations.

2.3. CuONPs synthesis

CuONPs were synthesized at 70°C using 1 mL aqueous extract of *C. sappan* and 19 mL of 10 mM $\text{CuSO}_4 \cdot 5\text{H}_2\text{O}$ solution under constant stirring at 500 rpm. To obtain suitable nanoparticles, an aqueous extract of *C. sappan* was added dropwise to the $\text{CuSO}_4 \cdot 5\text{H}_2\text{O}$ solution. After

30 min, the mixture was adjusted with 1 M NaOH or HCl to obtain pH 3, 6, 8, 10 and 12. Subsequently, the mixture was continuously reacted at 70°C for 2 h. The mixture was washed with Milli-Q water and any residual biological extract was removed by centrifugation at 8000× g for 30 min (three times). The obtained precipitate was dispersed in 10 mL of absolute ethanol and dried at 60°C for 8 h.

2.4. Characterizations of CuONPs

2.4.1. UV-visible spectroscopy

The dried powder of CuONPs was dispersed in Milli-Q water to obtain the concentration of 10 mg/mL. Then, 400 µL of this dispersion was diluted by adding 4 mL of Milli-Q water. The absorbance of this dilution was recorded from 200 to 800 nm using a UV-visible spectrophotometer (UV-2450 Shimadzu, Kyoto, Japan) to confirm the metal nanoparticles. Milli-Q water was used as a blank.

2.4.2. Fourier transform infrared (FTIR) spectroscopy

To explore the FTIR spectra of CuONPs, the dried powder of CuONPs was palletized with KBr. The obtained mixture was subjected to an FT-IR spectrometer (Thermo Nicolet/470FT-IR spectrometer, Nicolet Nexus, Madison, USA) in the range from 4000 to 500 cm⁻¹ at a resolution of 16 cm⁻¹.

2.4.3. Particle size and zeta potential analysis

The particle size, size distribution and the zeta potential of the synthesized CuONPs were measured *via* photon correlation spectroscopy (PCS) analysis using a Zetasizer Nano ZS (Malvern Instruments Company, Worcestershire, UK). The dispersion of CuONPs in Milli-Q water was prepared to a concentration of 1 mg/mL. The dispersion was diluted up to 10 times with Milli-Q water and subjected to sonication for 30 min before measurement. The hydrodynamic size and size distribution of the synthesized CuONPs were measured at a fixed angle of 173. The particle size was expressed as the average diameter in nm, whereas the particle size distribution was expressed as the polydispersity index (PDI). The zeta potential of the synthesized CuONPs was analyzed and automatically calculated based on the Smoluchowski equation (31) using the Zetasizer (Malvern Instruments Company) software version 7.1. All experiments were performed in triplicate.

2.4.4. Morphology and element composition

The morphology of CuONPs was investigated using a field emission scanning electron microscope (FE-SEM) (JSM 6335 F, JEOL Ltd, Tokyo, Japan). The

dried powder of CuONPs was mounted on a copper stub covered with carbon tape and sputter-coated with gold. The magnification was set at 30,000×. The shape and surface morphology of the particles were analyzed by secondary electron mode with an accelerating voltage of 0.3-30 kV. An energy-dispersive X-ray spectrophotometer (EDX) connected to the FE-SEM operated with a Si(Li) detector was used to analyze the CuONP composition and confirm the presence of copper.

2.5. Pathogenic strains and growth condition

In this study, *C. albicans* DMST 5815 was used as a pathogenic fungal strain. The strain was cultured in SDB at 37°C for 24-48 h. Fungal suspensions were prepared, and the cell concentration was adjusted to a turbidity of 0.5 McFarland standard using a McFarland densitometer (DEN-1 Biosan, Riga, Latvia).

2.6. Antifungal activity

The investigation of the antifungal activity of the synthesized CuONPs was performed by determining the minimum inhibitory concentration (MIC) and minimum fungicidal concentration (MFC) of the samples as follows. Stock dispersion of the synthesized CuONPs was prepared by dispersing dried powder of CuONPs in Milli-Q water to have a concentration of 12 mg/mL. Two-fold serial dilutions were prepared from the stock dispersion and 100 µL of each dilution was added to a 96-well microplate. Then, each well was added with 100 µL of *C. albicans* suspension in SDB at a concentration of 1 × 10⁵ CFU/mL. Therefore, each well contained *C. albicans* at 0.5 × 10⁵ CFU/mL and CuONPs at 6, 3, 1.5, 0.75, 0.375 and 0.187 mg/mL as final concentrations. The plate was incubated at 37°C for 24 h. The MIC is defined as the lowest concentration of CuONPs at which the microorganisms do not demonstrate visible growth. The turbidity in the well indicated the presence of microorganism growth. To determine MFC, the mixture in each well was streaked on each entire surface of SDA. Then, the agar plates were incubated in the same conditions as in the determination of MIC. After incubation, the lowest concentration of samples showing complete inhibition of *C. albicans* was recorded as MFC. All experiments were performed in triplicate. Nystatin solutions at concentrations of 0.012 × 10⁻⁴ - 2.5 × 10⁻³ mg/mL were used as positive controls.

2.7. Killing kinetics study

The study of killing kinetics of the synthesized CuONPs against *C. albicans* was conducted by adding 100 µL of CuONPs to a 96-well plate, followed by 100 µL of *C. albicans* suspension to obtain a final concentration of CuONPs at the lowest MFC and that of *C. albicans* concentration of 0.5 × 10⁵ CFU/mL. The plates were

incubated at 37°C for 8 h. At time intervals of 0, 30 min, 1, 2, 4, and 8 h, the mixtures were withdrawn, and viable cell counts were determined by plating 20 µL of known dilutions of the culture samples on the entire surface of SDA. The cell count plates were subsequently incubated at 37°C for 24 h. The plates with 30 to 300 colonies were used for CFU counts. Log CFU/mL was plotted against time for constructing the killing kinetics curves. Nystatin at MFC concentration was used as a positive control. All assays were analyzed in triplicate.

2.8. Antibiofilm assay

2.8.1. Biofilm formation inhibition

The effect of CuONPs on the biofilm formation of *C. albicans* was investigated as follows. CuONPs dispersions in Milli-Q water were prepared for various concentrations of CuONPs. Aliquots of 100 µL of these dispersions were added into 96-well plates, followed by adding 100 µL of the culture suspension to obtain the final CuONPs concentrations of 1/4 MFC, 1/2 MFC, and MFC and that of *C. albicans* of 0.5×10^6 CFU/mL. Nystatin solution in Milli-Q water at a final concentration of 1/4 MFC, 1/2 MFC, and MFC was used as a positive control, whereas the well without a sample was a negative control. After incubation at 37°C for 24 h, the supernatants were discarded and washed three times with phosphate buffer solution pH 7.4 (PBS) to remove non-adherent planktonic cells. The formed biofilm was stained with 200 µL of 0.1% (w/v) crystal violet in a plate at room temperature for 30 min. Then, the plate was washed three times with PBS in each well. Then the plate was added with 100 µL of 30% (v/v) acetic acid to dissolve the dye and further incubated for 15 min at room temperature. The adherence biofilm was quantified by measuring the OD at 595 nm using a microplate reader (Model 680, Bio-Rad, Hercules, California, USA). All experiments were done in triplicate. The percentage of biofilm inhibition of CuONPs was calculated by the following equation. Inhibition of biofilm formation (%) = $1 - (\text{OD}_{\text{sample}}/\text{OD}_{\text{control}}) \times 100$.

2.8.2. Eradication effect

The eradication effect of CuONPs on the formed biofilm was examined as follows. Suspension of *C. albicans* was prepared, and 100 µL of the culture suspension was added to a 96-well plate, followed by 100 µL of SDB to obtain the final culture concentration of 0.5×10^6 CFU/mL. After incubation for 24 h, the medium in each well was discarded. Then, 100 µL of SDB and 100 µL of CuONPs dispersion in Milli-Q water were added to obtain the final CuONPs concentration of MFC, 2 MFC and 4 MFC mg/mL. Nystatin in Milli-Q water at the same concentrations was used as a positive control, whereas the well without sample solution was a negative

control. The plates were further incubated at 37°C for 24 h. After incubation, the adherent candida cells were washed three times with PBS. The formed biofilm was stained with 200 µL of 0.1% (w/v) crystal violet for 30 min at room temperature. The plate was washed three times with PBS in each well. Then the plates were added 100 µL of 30% (v/v) acetic acid to dissolve the dye and incubated for 15 min at room temperature. The adherence biofilm was measured at 595 nm using a microplate reader (Model 680, Bio-Rad). The percentage of biofilm eradication was calculated by the following equation. Biofilm eradication (%) = $1 - (\text{OD}_{\text{sample}}/\text{OD}_{\text{control}}) \times 100$.

2.9. Confocal laser scanning microscopy (CLSM) analysis

The viable and dead cells in the biofilms were confirmed by CLSM (TCS SP8, Leica, Berlin, Germany). The suspension was prepared by mixing 1 mL of culture suspensions (1×10^6 CFU/mL) and 1 mL of SDB. The mixtures were added to six-well plates containing coverslips. The plates were incubated at 37°C for 48 h to allow the cells to form biofilms on the coverslips. After biofilm formation, the wells were rinsed with PBS. Then, 1 mL of SDB and 1 mL of CuONPs dispersion at the MFC concentration were added and the plates were further incubated at 37°C for 24 h. Nystatin in Milli-Q water at the MFC concentration was used as a positive control, whereas the well without sample was used as a negative control. After incubation, each well was washed 3 times with PBS to remove non-adherent *C. albicans*. Biofilm cell viability on the coverslips of each well was examined by a combination of fluorescent dyes mixed in a 1:1 volume ratio of 1.5 µM SYTO 9 for viable cells and 10 µM propidium iodide (PI) for dead cells. After incubation with the dye for 1 h, the coverslip was rinsed with PBS. The stained cell samples were examined with CLSM using $\lambda_{\text{ex/em}} = 488/543$ nm for SYTO 9 and $\lambda_{\text{ex/em}} = 522/590$ nm for PI.

2.10. Statistical analysis

Results were expressed as mean \pm SDs. Data from the biofilm assay were statistically analyzed using ANOVA followed by Duncan's post hoc test. A *p*-value < 0.05 was considered statistically significant.

3. Results

3.1. Synthesis of CuONPs

To study the effects of pH on CuONPs synthesis, the proportion of the aqueous extract of *C. sappan* and copper sulfate solution was fixed at 1:19 (v/v). The reaction temperature and duration were fixed at 70°C and 2.5 h, respectively. The reaction pHs of 3, 6, 8, 10 and 12 were studied. It was noted that the color of the aqueous

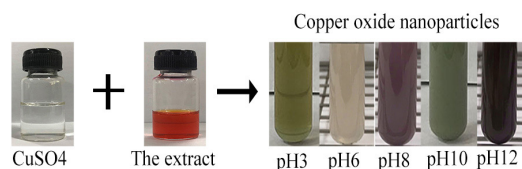


Figure 1. Photographs of CuONPs synthesized using *C. sappan* extract at different pH.

extract of *C. sappan* was orange, whereas that of copper sulfate solution was colorless. After adding the extract to the copper sulfate solution, the color of mixtures changed to gray. However, after adjusting the pH to 6, 8, 10, and 12, the mixtures changed to light purple, purple, light blue-green, and brownish black, respectively, as shown in Figure 1.

3.2. UV absorption and FTIR analysis

In the UV-visible spectroscopy analysis, the CuONPs synthesized at pH 6, 8, 10 and 12 exhibited a maximum absorbance peak of about 255 nm, as shown in Figure 2. It was found that the peak intensity increased while the pH increased. The CuONPs synthesized at pH 3 showed the small absorbance band at 224 nm. The FTIR spectra of the aqueous extract of *C. sappan* and the synthesized CuONPs are illustrated in Figure 3. The extract showed a broad peak at wave number region 3,500-3,300 cm^{-1} , which can be considered as OH stretching. Moreover, it showed the band in the region of 1,600-1,400 cm^{-1} which corresponds to C=O stretching of the carboxylic groups and the peak at 1,317 cm^{-1} which is due to C-O stretching. The FTIR spectra of the CuONPs synthesized at different pH showed different peak positions but in similar areas. The peaks at 3,479-3,387 cm^{-1} are considered for O-H stretching, the vibrations around 1,622-1,570 cm^{-1} are considered for C=O stretching, and around 1,131-1,121 cm^{-1} are for C-O vibration. In addition, the peaks at approximately 880-867 cm^{-1} are observed in the spectra of the CuONPs synthesized at pH 8, 10, and 12. These peaks are considered for aromatic Cu-O-H bonds. The peaks in the range of 520-623 cm^{-1} are considered for the expected cupric oxide and cuprous oxide vibrations.

3.3. Particle size and zeta potential analysis

The particle size of CuONPs synthesized at pH 6, 8, 10, and 12 was found in the range from approximately 255 to 458 nm with PDI range from 0.3 to 0.4, except for those synthesized at pH 3 that the obtained particles showed extremely large size and wide size distribution as shown in Table 1. The zeta potential of the synthesized particles at all pH values ranged from -13.93 to -25.0 mV, with pH 3 being the lowest and pH 10 and 12 being the highest values. It was noticed that the particle size and size distribution of CuONPs synthesized at pH 10 and 12

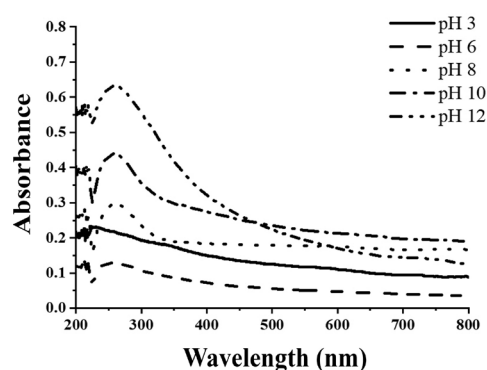


Figure 2. UV-visible spectra of CuONPs synthesized using *C. sappan* extract at different pH.

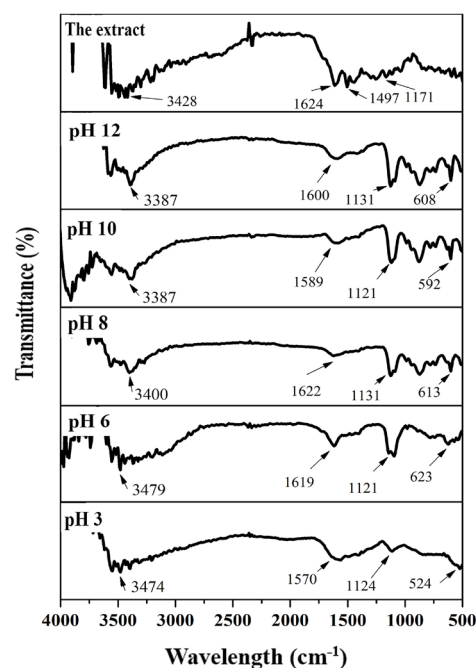


Figure 3. FTIR spectra of *C. sappan* extract and CuONPs synthesized using *C. sappan* extract at different pH.

Table 1. Particle size, size distribution, and zeta potential of the CuONPs synthesized at different pH of synthesis reaction

pH of synthesis reaction	Particle size (nm)	PdI	Zeta potential (mV)
pH 3	1322.3 ± 94.2 ^d	0.65 ± 0.11 ^b	-13.9 ± 0.2 ^c
pH 6	458.5 ± 6.9 ^e	0.38 ± 0.05 ^a	-15.7 ± 0.3 ^b
pH 8	369.4 ± 8.2 ^b	0.42 ± 0.02 ^a	-16.5 ± 0.1 ^b
pH 10	257.3 ± 8.4 ^a	0.32 ± 0.01 ^a	-24.8 ± 1.1 ^a
pH 12	255.6 ± 9.5 ^a	0.36 ± 0.06 ^a	-25.0 ± 0.2 ^a

Different letters indicate significant differences ($p < 0.05$) for particle size, PDI and zeta potential.

were significantly smaller and narrower than others.

3.4. SEM and EDX

The morphology and chemical compositions of the

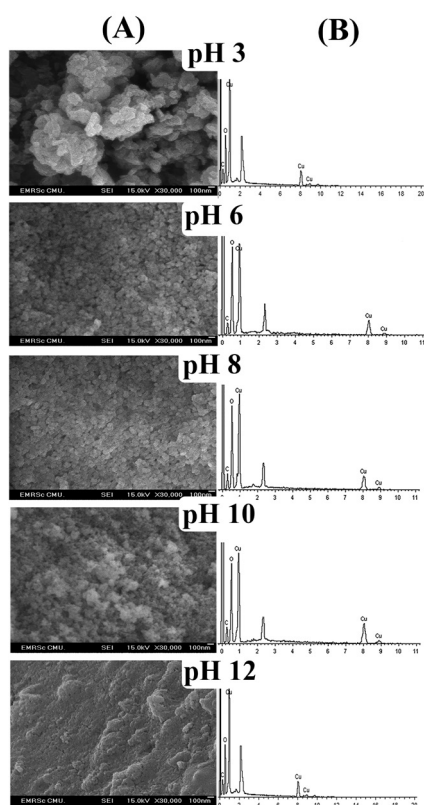


Figure 4. FESEM images (A) and EDX spectra (B) of CuONPs synthesized using *C. sappan* extract at different pH.

synthesized CuONPs investigated using SEM and EDX are shown in Figure 4. In the SEM images (Figure 4A), particle aggregation was observed in the CuONPs synthesized at pH 3, leading to extremely large particle sizes. Conversely, CuONPs synthesized at pH 6, 8, 10 and 12 had a spherical shape and overlapping of smaller particles. The EDX results (Figure 4B) of the CuONPs synthesized at all pH studied showed strong signals from elemental copper along with weak signals from other elements, such as oxygen and carbon.

3.5. Antifungal activity

The result of the antifungal test using the dilution method demonstrated that the CuONPs synthesized at various pH had antifungal activity but at different levels. As shown in Table 2, their MIC values ranged from 0.75-3 mg/mL, and MFC values were from 0.75 to more than 6 mg/mL. In the result, the MIC and MFC values of the CuONPs synthesized at pH 3 were the highest concentration, indicating the least antifungal effect on the pathogen. The MIC of the CuONPs synthesized at pH 8, 10 and 12 against the pathogen was the same value of 0.75 mg/mL. However, the MFC of the CuONPs synthesized at pH 8 was significantly higher than those synthesized at pH 10 and 12. This result suggested that the CuONPs synthesized at pH 10 and 12 were the most effective against *C. albicans*. Nystatin showed antifungal activity with MIC and MFC values of 4.9×10^{-3} and 19.5×10^{-3}

Table 2. Antifungal activity of the CuONPs synthesized at different pH of synthesis reaction

pH of synthesis reaction	MIC (mg/mL)	MFC (mg/mL)
pH 3	3.00	> 6.00
pH 6	1.50	3.00
pH 8	0.75	1.5
pH 10	0.75	0.75
pH 12	0.75	0.75
Nystatin	4.9×10^{-3}	19.5×10^{-3}

mg/mL, respectively.

3.6. Killing kinetics study

The microbial killing kinetics study measures the change in the *C. albicans* population within the time of specific exposure to the synthesized CuONPs. The growth curves of the samples compared to a negative control are presented in Figure 5. It was found that the growth curves of the pathogens after exposure to the CuONPs synthesized at pH 3, 6, and 8 were similar to that of the negative control. The reduction of viable cells could be found within 1-2 h, but after that the pathogen growth was significantly increased, whereas that synthesized at pH 10 and 12 could completely kill *C. albicans*. Interestingly, the CuONPs synthesized at pH 10 showed the completed killing of *C. albicans* within 1 h. The killing rate of these particles is as fast as that of nystatin, the positive control, and significantly faster than that synthesized at pH 12.

3.7. Antibiofilm assay

The result showed that the CuONPs synthesized in different pH could inhibit and eradicate biofilms of *C. albicans*, but at different levels, as shown in Figure 6. Furthermore, it was found that these effects depend on CuONPs concentration. For example, in Figure 6A, the inhibition effects of CuONPs synthesized at pH 3, 6, 8, 10, and 12 at 1/4 MFC were $8.95 \pm 5.21\%$, $12.54 \pm 9.93\%$, $27.55 \pm 4.92\%$, $38.05 \pm 0.87\%$ and $40.15 \pm 4.49\%$, respectively, while that of 1/2 MFC were $20.24 \pm 0.36\%$, $48.46 \pm 2.21\%$, $48.26 \pm 3.11\%$, $69.99 \pm 3.16\%$ and $43.05 \pm 5.93\%$, respectively. It was found that CuONPs synthesized at pH 6, 8, 10, and 12 at the MFC were able to inhibit biofilm formation by more than 70%. Interestingly, at this concentration, CuONPs synthesized at pH 10 and 12 showed the biofilm inhibition effect of $86.10 \pm 1.10\%$ and $87.68 \pm 0.47\%$, respectively, significantly higher than that of nystatin at its MFC. In Figure 6B, the effects of the synthesized CuONPs on biofilm eradication are shown. The results showed that after exposure to the synthesized CuONPs, the formed biofilm of *C. albicans* was approximately $27.05 \pm 4.25\%$ to $79.28 \pm 2.28\%$ eliminated. The efficiency of the CuONPs synthesized at all tested pHs,

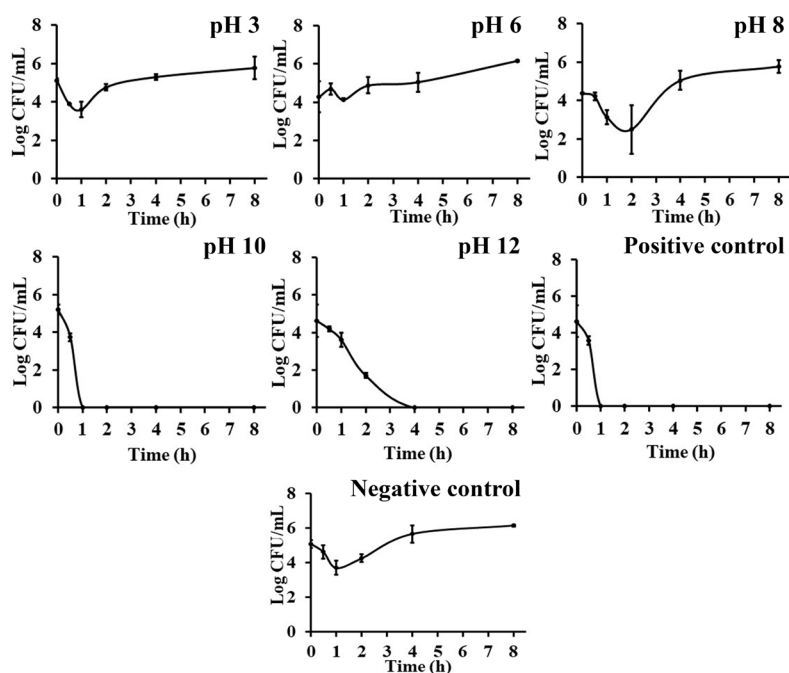


Figure 5. Time-killing kinetics against *C. albicans* of CuONPs synthesized using *C. sappan* extract at different pH in comparison with nystatin.

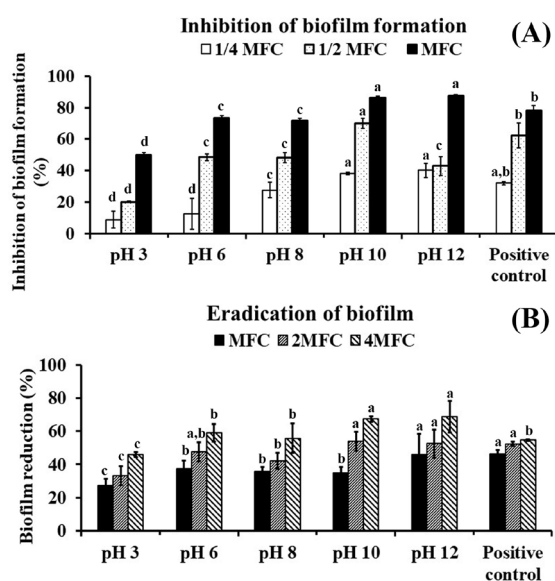


Figure 6. Effects of CuONPs synthesized using *C. sappan* extract at different pH in comparison with nystatin on inhibition of biofilm formation (A) and biofilm eradication (B). Different letters indicate significantly different ($p < 0.05$) for quantitative percentage of biofilm inhibition and biofilm eradication in the same sample concentration.

at MFC was less than 50%, while at 2 MFC, the biofilm eradication efficiency of the CuONPs synthesized at pH 10 and 12 was above 50% ($53.88 \pm 5.79\%$ and $52.52 \pm 8.63\%$, respectively). At the highest test concentration (4 MFC), the CuONPs synthesized at pH 6, 8, 10 and 12 showed a greater than 50% reduction in biofilm, whereas those synthesized at pH 3 showed only $46.03 \pm 1.47\%$ reduction. Based on these results, CuONPs synthesized at pH 10 and 12 were considered to have significantly higher potential for inhibition and removal of *C. albicans* biofilm than those synthesized at other pHs and nystatin.

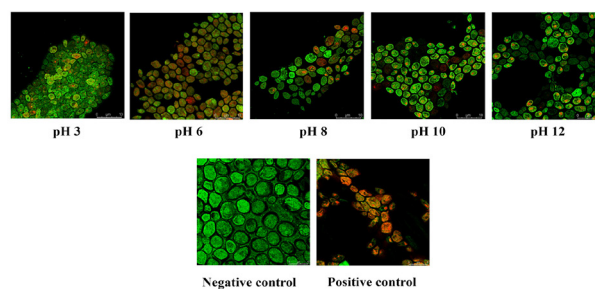


Figure 7. CSLM images of *C. albicans* biofilm treated with CuONPs synthesized using *C. sappan* extract at different pH in comparison with nystatin.

3.8. CLSM analysis

CLSM images of *C. albicans* biofilms, as in Figure 7, showed the dead cells in red color and live cells in green color. The red cells stained with PI demonstrated that the number of cells after exposure to the synthesized CuONPs and the nystatin-positive control was higher than that of the negative control. After exposure to the CuONPs synthesized at all pH values and the nystatin-positive control, few green spots of viable cells were detected. After treatment with the synthesized CuONPs, the viable cell population was obviously lower than that of the negative control group. The population of *C. albicans* cells in the biofilms after exposure to the CuONPs synthesized at pH 10 and 12 was less than the others suggesting that most cells were dead and washed off the films.

4. Discussion

Many millions of people are affected by antimicrobial

resistance pathogens and many of them die every year (32). *C. albicans* represents the predominant cause of fungal infections and has the ability to develop biofilms that protect the pathogenic cells inside and increase their resistance to antifungal drugs (1,2). The use of metal nanoparticles is an effective alternative against antimicrobial-resistant pathogenic strains. We are interested in CuONPs because of its wide range of applications. It also has high antimicrobial activity against *C. albicans* and other pathogens (33).

Several methods such as electrochemical (34), radiation (35), photochemical (36), and by biological methods (37) have been used to synthesize metal nanoparticles. This study focuses on biological methods as it aims to reduce the use of inorganic substances. In this method, chemical reducing agents are replaced by high reducing power plant extract. *C. sappan* extract was used due to its high reducing activity (38). The different colors of the synthesized metal nanoparticles are due to the surface plasmon resonance excitation, a signal of nanoparticle formation (39). The surface plasmon resonance is due to the presence of free electrons, which is formed by conduction and valence bands, as they are close together in metals (40). Our results show different colors of the CuONPs system synthesized at different pH suggesting that pH affects the surface plasma resonance of the end products. Oligomeric clusters of copper can absorb at wavelength range 250-300 nm (41). Our results are in good agreement that the obtained CuONP particles absorb the wavelength range of 220-255 nm depending on the pH. The different absorption peaks of CuONPs synthesized at various pH values confirm the effect of pH on the surface plasma resonance absorbance of the obtained metal nanoparticles. It was found that the intensity of the absorbance peak of the obtained CuONP was increased by increasing the pH of the synthesis reaction. This might be related to the higher rate of formation of CuONPs in alkaline pH due to the ionization of the phenolic functional group present in the extract. The FTIR spectra of all CuONPs matched the FTIR spectra of the *C. sappan* extract. The obtained results reliably confirmed that the organic compounds of the *C. sappan* extract were responsible for the reduction of copper ions to CuONPs. The characteristic band at 528 cm^{-1} present in the FTIR spectra of CuONPs was considered to be that of cupric oxide (42). The negative value of zeta potential of the obtained CuONPs was attributed to a group of negatively charged compounds in the *C. sappan* extract. Our results showed that the small-size nanoparticles with high negative zeta potential could be synthesized only at pH 10 and 12. The size of the CuONPs synthesized at pH lower than 10 was large due to the low zeta potential, thus, leading to high particle aggregation. These can be confirmed by SEM images of CuONPs, showing minimal particle aggregation from the preparations at pH 10 and 12 and the highest particle aggregation from the preparation at pH 3. From the

above findings, it can be concluded that the pH of the green synthesis reaction is an important factor for the characteristics of the obtained metal nanoparticles.

For antifungal activity, the smaller particles of CuONPs showed higher activity against *C. albicans* than larger particles. It has been reported that CuONPs involved in inactivation of *Escherichia coli* through membrane damage, intracellular ROS generation, and inactivation of fumarase enzyme (43). For the inhibition of *C. albicans*, we consider that CuONPs can destroy fungal membranes by the released Cu ion from the nanoparticles. In general, antifungal agents are classified as fungicidal and fungistatic according to the ratio of MFC to MIC. If the MFC/MIC ratio is ≤ 4 , the agent is considered to have fungicidal activity. If the MFC/MIC ratio is > 4 , the agent is fungistatic activity (44). From our results, the CuONPs synthesized at pH 6, 8, 10 and 12 possess fungicidal activity while the antifungal activity of those synthesized at pH 3 is fungistatic. This is considered that the smaller particle size has a more powerful antifungal effect.

The study of killing kinetics is to confirm the fungicidal activity of the agents and the results are more clinically useful than static MFC alone (45). It has been reported that fungicidal agent should be able to completely kill the test organisms within 24 h (46). In the present study, the CuONPs synthesized at different pH showed different killing efficiency. The CuONPs synthesized at pH 10 and 12 can completely kill *C. albicans* within less than 1 and 4 h, respectively, suggesting that these CuONPs are fungicidal agent.

Biofilms of human pathogens have been found to be highly associated with patient morbidity and mortality. It has been reported that the *Candida* spp. can form polymeric biofilms that can enhance the adherence of the pathogens to the surface (47). In addition, the extracellular polymeric substances secreted by *C. albicans* can prevent the diffusion of any agents into the cells, leading to high resistance to many antifungal drugs (48). Therefore, the prevention and eradication of biofilms are of great importance in the treatment of fungal infections. In this study, CuONPs synthesized at all pH exhibited a dose-dependent effects of inhibition of biofilm formation and removal of the formed biofilms of *C. albicans* but different levels. CuONPs synthesized at pH 10 and 12 showed the highest efficiency in these activities. The antibiofilm activities can be confirmed by CLSM analysis using fluorescent stains. Red fluorescence of PI indicates cells with damaged membranes and stains DNA of the dead cells, whereas green fluorescence of SYTO 9 indicates cells with intact membranes of viable cells. Our results in CLSM images show several viable cells in the biofilm of the untreated group. While viable cells were dramatically reduced in the synthesized CuONPs-treated biofilms. This indicates that CuONPs can effectively destroy *C. albicans*. These results are consistent with previous study where

CuONPs synthesized using leaf extracts of *Camellia japonica* showed a reduction in the number of colonies of *Pseudomonas aeruginosa* and *Klebsiella pneumoniae* (49). Our study also shows that many dead cells remain and can be clearly seen in the CLSM image of CuONPs synthesized at pH 3. However, for those synthesized at higher pH, especially at pH 10 and 12, only a small number of dead cells can be seen. This assumes that most dead cells are easily washed away.

In conclusion, the findings in this study confirmed that CuONPs biosynthesized using *C. sappan* extract at pH 10 and 12 possessed potent antifungal and antibiofilm activity. The results suggest that the obtained CuONPs may be a promising antifungal agent and are suitable for further study in animal models and clinical trials.

Acknowledgements

The authors greatly appreciate HISTOCENTER (Thailand) Co., Ltd. for providing us with CLSM analysis. We would like to thank the Center of Excellent in Pharmaceutical Nanotechnology of Chiang Mai University for facility support.

Funding: This work was supported by a grant from Thailand Research Fund through the Research and Researcher for Industry (RRI) Grant number PHD59I0076.

Conflict of Interest: The authors have no conflicts of interest to disclose.

References

- Sandai D, Tabana YM, El Ouweini A, Ayodeji IO. Resistance of *Candida albicans* biofilms to drugs and the host immune system. *Jundishapur J Microbiol.* 2016; 9:1-7.
- Eshima S, Kurakado S, Matsumoto Y, Kudo T, Sugita T. *Candida albicans* promotes the antimicrobial tolerance of *Escherichia coli* in a cross-kingdom dual-species biofilm. *Microorganisms.* 2022; 10:2179-2192.
- Hawser SP, Douglas LJ. Resistance of *Candida albicans* biofilms to antifungal agents *in vitro*. *Antimicrob Agents Chemother.* 1995; 39:2128-2131.
- Lalla RV, Latortue MC, Hong CH, Ariyawardana A, D'Amato-Palumbo S, Fischer DJ, Martof A, Nicolatou-Galitis O, Patton LL, Elting LS, Spijkervet FKL, Brennan MT. A systematic review of oral fungal infections in patients receiving cancer therapy. *Support Care Cancer.* 2010; 18:985-992.
- Yoshijima Y, Murakami K, Kayama S, Liu D, Hirota K, Ichikawa T, Miyake Y. Effect of substrate surface hydrophobicity on the adherence of yeast and hyphal *Candida*. *Mycoses.* 2010; 53:221-226.
- Garcia-Cuesta C, Sarrion-Pérez MG, Bagán JV. Current treatment of oral candidiasis: A literature review. *J Clin Exp Dent.* 2014; 6:576-582.
- Gleiznys A, Zdanavičienė E, Žilinskas J. *Candida albicans* importance to denture wearers. A literature review. *Stomatologija.* 2015; 17:54-66.
- Azharuddin M, Zhu GH, Das D, Ozgur E, Uzun L, Turner APF, Patra HK. A repertoire of biomedical applications of noble metal nanoparticles. *Chem Commun.* 2019; 5:6964-6996.
- Dharmadasa R, Jha M, Amos DA, Druffel T. Room temperature synthesis of a copper ink for the intense pulsed light sintering of conductive copper films. *ACS Appl Mater Interfaces.* 2013; 5:13227-13234.
- Gawande MB, Goswami A, Felpin FX, Asefa T, Huang X, Silva R, Zou X, Zboril R, Varma RS. Cu and Cu-based nanoparticles: Synthesis and applications in catalysis. *Chem Rev.* 2016; 116:3722-3811.
- Sharma H, Mishra PK, Talegaonkar S, Vaidya B. Metal nanoparticles: A theranostic nanotool against cancer. *Drug Discov Today.* 2015; 20:1143-1151.
- Ahamed M, Alhadlaq HA, Khan MAM, Karuppiah P, Al-Dhabi NA. Synthesis, characterization, and antimicrobial activity of copper oxide nanoparticles. *J Nanomater.* 2014; 2014:1-4.
- Hardie JM. Oral microbiology: Current concepts in the microbiology of dental caries and periodontal disease. *Br Dent J.* 1992; 172:271-278.
- Rahimi G, Khodavandi A, Yaghoobi R. Antimycotic effect of copper oxide nanoparticles on *Candida albicans* biofilm. *J Micro Nano Biomed.* 2016; 1:7-12.
- Tinkle S, Mcneil SE, Mühlebach S, Bawa R, Borchard G, Barenholz YC, Tamarkin L, Desai N. Nanomedicines: Addressing the scientific and regulatory gap. *Ann N Y Acad Sci.* 2014; 1313:35-56.
- Nabila MI, Kannabiran K. Biosynthesis, characterization and antibacterial activity of copper oxide nanoparticles (CuO NPs) from actinomycetes. *Biocatal Agric Biotechnol.* 2018; 15:56-62.
- Amin F, Fozia, Khattak B, Alotaibi A, Qasim M, Ahmad I, Ullah R, Bourhia M, Gul A, Zahoor S, Ahmad R. Green synthesis of copper oxide nanoparticles using *Aerva javanica* leaf extract and their characterization and investigation of *in vitro* antimicrobial potential and cytotoxic activities. *Evid Based Complement Alternat Med.* 2021; 2021:1-12.
- Suwan T, Khongkhunthian S, Okonogi S. Silver nanoparticles fabricated by reducing property of cellulose derivatives. *Drug Discov Ther.* 2019; 13:70-79.
- Mohanpuria P, Rana NK, Yadav SK. Biosynthesis of nanoparticles: Technological concepts and future applications. *J Nanoparticle Res.* 2008; 10:507-517.
- Mittal AK, Chisti Y, Banerjee UC. Synthesis of metallic nanoparticles using plant extracts. *Biotechnol Adv.* 2013; 31:346-356.
- Andra S, Balu SK, Jeevanandham J, Muthalagu M, Vidyavathy M, Chan YS, Danquah MK. Phytosynthesized metal oxide nanoparticles for pharmaceutical applications. *Naunyn Schmiedeberg Arch Pharmacol.* 2019; 392:755-771.
- Mohamed EA. Green synthesis of copper & copper oxide nanoparticles using the extract of seedless dates. *Heliyon.* 2020; 6:1-6.
- Siddiqui VU, Ansari A, Chauhan R, Siddiqui WA. Green synthesis of copper oxide (CuO) nanoparticles by *Punica granatum* peel extract. *Mater Today Proc.* 2019; 36:751-755.
- Nirmal NP, Rajput MS, Prasad RGSV, Ahmad M. Brazilin from *Caesalpinia sappan* heartwood and its pharmacological activities: A review. *Asian Pac J Trop Med.* 2015; 8:421-430.

25. Srinivasan R, Selvam GG, Karthik S, Mathivanan K, Baskaran R, Karthikeyan M, Gopi M, Govindasamy C. *In vitro* antimicrobial activity of *Caesalpinia sappan* L. Asian Pac J Trop Biomed. 2012; 2:136-139.
26. Wu SQ, Otero M, Unger FM, Goldring MB, Phrutivorapongkul A, Chiari C, Kolb A, Viernstein H, Toegel S. Anti-inflammatory activity of an ethanolic *Caesalpinia sappan* extract in human chondrocytes and macrophages. J Ethnopharmacol. 2011; 138:364-372.
27. Badami S, Moorkoth S, Rai SR, Kannan E, Bhojraj S. Antioxidant activity of *Caesalpinia sappan* heartwood. Biol Pharm Bull. 2003; 26:1534-1537.
28. Nirmal NP, Rajput MS, Prasad RGS V, Ahmad M. Brazilin from *Caesalpinia sappan* heartwood and its pharmacological activities : A review. Asian Pac J Trop Med. 2015; 8:421-430.
29. Salayov A, Bedlovičová Z, Daneu N, Baláz M, Bujňáková ZL, Balázová L, Tkáčiková L. Green synthesis of silver nanoparticles with antibacterial activity using various medicinal plant extracts: Morphology and antibacterial efficacy. Nanomaterials. 2021; 11:1005-1025.
30. Patra JK, Baek KH. Green nanobiotechnology: Factors affecting synthesis and characterization techniques. J. Nanomater. 2014; 2014:1-12.
31. Rizvi SAA, Saleh AM. Applications of nanoparticle systems in drug delivery technology. Saudi Pharm J. 2018; 26:64-70.
32. Raut S, Adhikari B. The need to focus China's national plan to combat antimicrobial resistance. Lancet Infect Dis. 2017; 17:137-138.
33. Azam A, Ahmed AS, Oves M, Khan MS, Memic A. Size-dependent antimicrobial properties of CuO nanoparticles against Gram-positive and -negative bacterial strains. Int J Nanomedicine. 2012; 7:3527-3535.
34. Raja M. Production of copper nanoparticles by electrochemical process. Powder Metall Met Ceram. 2008; 47:402-405.
35. Hori T, Nagata K, Iwase A, Hori F. Synthesis of Cu nanoparticles using gamma-ray irradiation reduction method. Jpn J Appl Phys. 2014; 53:1-5.
36. Giuffrida S, Costanzo LL, Ventimiglia G, Bongiorno C. Photochemical synthesis of copper nanoparticles incorporated in poly(vinyl pyrrolidone). J Nanoparticle Res. 2008; 10:1183-1192.
37. Lee HJ, Song JY, Kim BS. Biological synthesis of copper nanoparticles using *Magnolia kobus* leaf extract and their antibacterial activity. J Chem Technol Biotechnol. 2013; 88:1971-1977.
38. Suwan T, Wanachantararak P, Khongkhunthian S, Okonogi S. Antioxidant activity and potential of *Caesalpinia sappan* aqueous extract on synthesis of silver nanoparticles. Drug Discov Ther. 2018; 12:259-266.
39. Sathiyavimal S, Vasantharaj S, Bharathi D, Saravanan M, Manikandan E, Kumar SS, Pugazhendhi A. Biogenesis of copper oxide nanoparticles (CuONPs) using *Sida acuta* and their incorporation over cotton fabrics to prevent the pathogenicity of Gram negative and Gram positive bacteria. J Photochem Photobiol B. 2018; 188:126-134.
40. Jana J, Ganguly M, Pal T. Enlightening surface plasmon resonance effect of metal nanoparticles for practical spectroscopic application. RSC Adv. 2016; 6:86174-86211.
41. Khatouri J, Mostafavi M, Amblard J, Belloni J. Radiation-induced copper aggregates and oligomers. Chem Phys Lett. 1992; 191:351-356.
42. Ethiraj AS, Kang DJ. Synthesis and characterization of CuO nanowires by a simple wet chemical method. Nanoscale Res Lett. 2012; 7:1-5.
43. Meghana S, Kabra P, Chakraborty S, Padmavathy N. Understanding the pathway of antibacterial activity of copper oxide nanoparticles. RSC Adv. 2015; 5:12293-12299.
44. Dudiuk C, Berrio I, Leonardelli F, Morales-Lopez S, Theill L, Macedo D, Yesid-Rodriguez J, Salcedo S, Marin A, Gamarra S, Garcia-Effron G. Antifungal activity and killing kinetics of anidulafungin, caspofungin and amphotericin B against *Candida auris*. J Antimicrob Chemother. 2019; 74:2295-2302.
45. Keepers TR, Gomez M, Celeri C, Nichols WW, Krause KM. Bactericidal activity, absence of serum effect, and time-kill kinetics of ceftazidime-avibactam against β -lactamase-producing *Enterobacteriaceae* and *Pseudomonas aeruginosa*. Antimicrob Agents Chemother. 2014; 58:5297-5305.
46. Pfaller MA, Sheehan DJ, Rex JH. Determination of fungicidal activities against yeasts and molds: Lessons learned from bactericidal testing and the need for standardization. Clin Microbiol Rev. 2004; 17:268-280.
47. Forsberg K, Woodworth K, Walters M, Berkow EL, Jackson B, Chiller T, Vallabhaneni S. *Candida auris*: The recent emergence of a multidrug-resistant fungal pathogen. Med Mycol. 2019; 57:1-12.
48. Chandra J, Mukherjee PK, Leidich SD, Faddoul FF, Hoyer LL, Douglas LJ, Ghannoum MA. Antifungal resistance of Candidal biofilms formed on denture acrylic *in vitro*. J Dent Res. 2001; 80:903-908.
49. Rajivgandhi G, Maruthupandy M, Muneeswaran T, Ramachandran G, Manoharan N, Quero F, Anand M, Song JM. Biologically synthesized copper oxide nanoparticles enhanced intracellular damage in ciprofloxacin resistant ESBL producing bacteria. Microb Pathog. 2019; 127:267-276.

Received May 11, 2023; Revised August 19, 2023; Accepted August 19, 2023.

*Address correspondence to:

Siriporn Okonogi, Center of Excellent in Pharmaceutical Nanotechnology, Faculty of Pharmacy, Chiang Mai University, Chiang Mai 50200, Thailand.
E-mail: okng2000@gmail.com

Released online in J-STAGE as advance publication August 24, 2023.